Article Title: Enhanced protein synthesis is a defining requirement for neonatal B cell development

Running title: Translation dictates neonatal B lymphopoiesis

Hugo Åkerstrand[1], Elena Boldrin[1], Giorgia Montano[1], Stijn Vanhee[1], Karin Olsson[1], Niklas Krausse[1], Stefano Vergani[1], Maciej Cieśla[2], Cristian Bellodi[2], Joan Yuan[1*]

[1] Developmental Immunology Unit, Department of Molecular Hematology, Lund Stem Cell Center, Lund University, Lund, Sweden
[2] RNA and Stem Cell Biology Unit, Department of Molecular Hematology, Lund Stem Cell Center, Lund University, Lund, Sweden

*** Correspondence**:
Joan Yuan
joan.yuan@med.lu.se

Manuscript length
Number of words: 5006
Number of Figures: 5
Number of Supplemental Figures: 2
Number of Supplemental Tables: 2

Keywords
Lin28b, protein synthesis, B-1 cells, neonatal B cell development, c-MYC

Abstract

Protein synthesis is a stringently regulated process that fundamentally dictates capacity for cellular growth. Rapid fluctuations in cell size and proliferation mark the developmental transitions between B cell precursor stages. However, little is known about how ribosomal control may impact this process. Here, we identify elevated protein synthesis as a defining feature of early-life B cell development and a determinant for the output of self-reactive CD5+ B-1a cells in mice. The LIN28B heterochronic RNA binding protein is a key molecular regulator of fetal and neonatal B lymphopoiesis and can reinitiate B-1a cell generation when ectopically expressed in adult hematopoiesis. Interactome analyses in primary B cell precursors showed direct binding of LIN28B to ribosomal protein transcripts, which correlated with their elevated protein expression *in vivo*. Genetic perturbations demonstrated that LIN28B is necessary and sufficient to promote enhanced protein synthesis during the small Pre-B and immature B cell stages. Furthermore, subdued protein synthesis in a ribosomal hypomorphic mouse model was detrimental for neonatal B lymphopoiesis and the output of B-1a cells, without affecting B cell development in the adult at steady state. Finally, Rapamycin treatment inhibited LIN28B induced positive selection of self-reactive CD5+ immature B cells destined for the B-1a lineage. Taken together, our results identify elevated protein synthesis as a key mechanism for LIN28B induced B cell development and the generation of B-1a cells early in life.

Introduction

B-cell development is centered around alternating stages of cellular proliferation and V(D)J recombination at the immunoglobulin heavy and light chain loci, with the goal of producing a diverse yet self-tolerant B cell repertoire. During the Pro-B cell stage, productive IgH rearrangement results in the expression of a pre-BCR complex and differentiation into the large Pre-B cell stage. The latter is marked by a transient burst of clonal expansion. Cell cycle exit is accompanied by the initiation of light chain recombination and entry into the small Pre-B cell stage. IL-7 signaling is an essential trophic factor during the Pro- and large Pre-B cell stages, promoting cell survival, proliferation, and differentiation, through distinct effects mediated by the Stat5 and mTORC1/c-MYC signaling axes (1, 2). IL-7 signaling wanes as large Pre-B cells move away from IL-7 producing stromal cells in vivo and its attenuation is required for the developmental progression into the small Pre-B cell stage and the onset of IgK light chain recombination (3). Generation of a productive immunoglobulin heavy and light chain complex leads to membrane IgM expression and developmental progression into the immature B (Imm-B) cell stage. Here, cells carrying innocuous BCRs are allowed to mature while self-reactive specificities are subject to central tolerance mechanisms including receptor editing and apoptosis to remove potentially harmful recognition of "self" (4). Progression through these stages is accompanied by dramatic fluctuations in bioenergetic states. Although metabolic capacity has been proposed to modulate the central tolerance checkpoint (5), this theory has not been empirically proven.

Much of what we know about B cell development comes from studies in adult mice, which differs significantly from fetal and neonatal life. For example, while B cell development in adult bone marrow strictly requires IL-7 mediated signaling, B cell output can take place in neonatal mice lacking IL-7Ra until around two weeks of age (6). Furthermore, both the pre-BCR and mature BCR checkpoints are less stringent during neonatal life allowing for the positive selection of poly and self-reactive specificities in mice and men (7-9). This correlates with the output of self-reactive CD5+ B-1a cells in mice, which secrete natural antibodies important for the clearance of cellular debris and act as a first line of defense against pathogens (10). Despite these differences, the basis for the developmental switch in B cell output is not well understood.

One molecular program that distinguishes early life lymphopoiesis is centered around the post-transcriptional regulator LIN28B. It is one of two mammalian homologs of *lin-28* first identified in *Caenorhabditis elegans* to encode a heterochronic RNA binding protein in control of the timing of larval development (11). In the mammalian hematopoietic system, *Lin28b* expression is abundant during fetal life and gradually silenced within the first two to three weeks of life, critically controlling a neonatal switch in hematopoietic stem cell function and lineage output patterns (12). Like its mammalian paralog *Lin28a*, *Lin28b* plays an established role in regulating organismal growth and cellular metabolism, most famously through the direct inhibition of the biogenesis of the evolutionarily conserved Let-7 family of microRNAs. LIN28A/B expression de-represses Let-7 targets which include the proto-oncogenes *Myc*, *Arid3a*, *Hmga2* and *Igf2bp1-3* (13-15). We and others have previously shown that ectopic

LIN28A/B expression in the adult promotes key aspects of fetal-like lymphopoiesis, including the efficient production of CD5+ B-1a cells (13, 16-18). Furthermore, studies from both BCR poly-clonal and transgenic mouse models make clear that LIN28B relaxes the central tolerance checkpoint to allow for the positive selection of self-reactive BCR specificities and thereby uniquely shapes the neonatal B cell repertoire (19, 20). Immunophenotypically, this phenomenon is marked by the developmental progression of CD5+ imm-B cells destined for the B-1a cell lineage (19). The mechanism for this effect is, although not fully understood, at least in part linked to augmentation of c-MYC protein levels in Imm-B cells and the CD19/PI3K/c-MYC positive feedback loop (19) known to promote B cell positive selection (21).

A less understood mechanism of LIN28B action is through the direct binding of coding mRNAs to either positively or negatively regulate transcript stability and protein translation, in a context dependent manner (22-31). In particular, several studies have demonstrated the ability of LIN28B to promote the translation of ribosomal proteins, through Let-7 independent direct binding to their transcripts in human ES cells (32), transformed human kidney (22) and neuroblastoma (31) cell lines. However, the role of the protein synthesis pathway in LIN28B dependent B cell positive selection is not known. Here we demonstrate that LIN28B directly interacts with ribosomal protein transcripts in primary B cell precursors. Importantly, LIN28B expression is necessary and sufficient to elevate protein synthesis specifically during the later stages of IL-7 independent bone marrow B cell maturation. Finally, we show that an augmented mode of protein synthesis is a hallmark of neonatal B cell development and a pre-requisite for the positive selection of CD5+ Imm-B cells and the output of B-1a cells early in life. We conclude that LIN28B augments protein synthesis to support neonatal B cell output.

Materials and methods

Mice

tet-LIN28B mice were generated by intercrossing *Col1a*$^{tetO\text{-}LIN28B}$ (The Jackson Laboratory, #023911) to *Rosa26*^{rtTA*m2} (The Jackson Laboratory, #006965) mice and were originally obtained from the laboratory of George Daley (Harvard Medical School) (33). Monoallelic transgene expressing mice were used for experiments. *Rosa26*^{rtTA*m2} heterozygous littermates were used as control mice. For *in vivo* experiments, Doxycycline (Dox) chow (200 mg/kg, Ssnif, cat#A112D70203) was fed to tet-LIN28B and littermates for 10 days before analysis. B6.Cg-*Lin28b*$^{tm1.1Gqda}$/J (*Lin28b* KO) (The Jackson Laboratory, #023917) and C57BLKS-*Rpl24*^{Bst}/J (Bst) (The Jackson Laboratory, #000516) were originally purchased from the Jackson laboratory. Wildtype mice were originally purchased from Taconic (B6NTAC, Taconic). The *Lin28b*-eGFP knock-in strain was generated as previously described (34). Adult mice were used at 10 to 16 weeks of age, neonates were analyzed at the indicated days post-birth. Male and female mice were used interchangeably throughout the experiments. Animal husbandry and experimental procedures were performed in accordance with ethical permits issued by the Swedish Board of Agriculture.

Bone marrow cultures

Adult bone marrow B cell precursors from untreated adult mice were expanded and enriched *ex vivo*, as previously described (35). Briefly, single cell suspension of red blood cell lysed bone marrow was plated in pre-warmed RPMI-1640 (Fischer Scientific, cat#21875091) and incubated for 15 min at 37 ºC. The non-adherent cells were isolated and seeded at a cell density of 0.75-1.5 million/mL using fully supplemented RPMI-1640, IL-7 (20 ng/mL, Peprotech, cat#217-17), and Dox (0.1 µg/ml, Sigma-Aldrich, cat#D3072). Dox treatment for bone marrow cultures was always initiated at the start of the culture, never *in vivo*. The cell culture medium was refreshed every second day.

RNA Immunoprecipitation Sequencing (RIP-seq)

Cells from day 5 bone marrow cultures from tet-LIN28B or littermate control mice were used for lysis and RIP using Magna RIP RNA-Binding Protein Immunoprecipitation kit (Millipore, cat#17-700) according to the manufacturer's instructions. Briefly, 10% of the total lysate was kept as input sample. 4 µg of anti-Flag antibody (Sigma) and 50 µl of A/G beads (Millipore, cat#16-663) were added to the lysate and incubated for 3 hours. Beads were washed 6 times with ice-cold RIP wash buffer (Millipore, cat#17-700). RNA was extracted using RNAzol (Sigma-Aldrich, cat#R4533) and Direct-zol RNA MicroPrep kit (Zymo Research, cat#R2060). For RNA quantification and quality control respectively, Qubit with RNA HS kit (Thermofisher Scientific, cat# Q32852) and Agilent Bioanalyzer with RNA Pico kit (Agilent, cat#5067-1513) were used according to the manufacturer's instructions. 20ng of total RNA was used for the cDNA synthesis and amplification with the SMART-Seq v4 Ultra Low Input RNA Kit for Sequencing (Takara, cat#634889) according to instructions. Library tagmentation and indexing was performed using Nextera XT DNA Kit (Illumina, cat#FC-121-1030) and Nextera XT v2 set A Indexing kit (Illumina, cat#15052163). Library quantification and library size were measured using Qubit DNA HS kit (Thermofisher Scientific, cat#Q32851) and

155 BioAnalyzer DNA HS kit (Agilent, cat#5067-4626). The samples were run in NextSeq 550
156 using NextSeq High output 150 cycles 2x76bp. Reads were aligned using STAR aligner v2.7.1
157 to mm10 and counted using RSEM v1.28. Genes were filtered for an FPKM of at least 50 in
158 total tet-LIN28B input samples and following LIN28B immunoprecipitation. Enrichment was
159 calculated as IP over Input FPKM for each of the two tet-LIN28B samples individually. 238
160 transcripts had an average enrichment of at least 2-fold and were considered for subsequent
161 analyses. Littermate control sample was not considered when generating this list. Gene
162 ontology analysis was done using the Panther database (pantherdb.org, release 17.0). Data is
163 accessible through GEO, GSE217788.
164
165 **RNA sequencing**
166 B cell precursor subsets were FACS sorted from adult BM of Dox induced mice of the indicated
167 genotypes. RNA sequencing libraries were generated as previously described (19) and
168 sequenced on Illumina NextSeq and NovaSeq. Note that FSC-A low, small Pro-B cells were
169 excluded from the FACS sorting gate. All data was processed and analyzed as previously
170 described (19). Data is accessible through GSE217788 except for Imm-B that was previously
171 generated (19) and is accessible through GSE135603. GSEA used Wald's stat as ranking
172 metric. MSigDB Mouse collections Hallmark_MYC_target_v1 and MirDB
173 CTACCTC_LET7A_LET7B_LET7C_LET7D_LET7E_LET7F_MIR98_LET7G_LET7I
174 gene sets were used for GSEA.
175
176 **Metabolic labeling of nascent proteins**
177 Cells were depleted of endogenous methionine by pre-culturing them in methionine free RPMI
178 (Fisher Scientific, cat#A1451701). After 45 minutes, the medium was supplemented with L-
179 azidhomoalanine (AHA, 1 mM final concentration, Fisher Scientific, cat#C10102) and labeled
180 for one hour. AHA uptake was visualized using Click-iT Plus Alexa Fluor 555 Picolyl Azide
181 Toolkit (Fisher Scientific, cat#C10642), following the manufacturer's protocol. Briefly, up to
182 3 x 10^6 cells were fixed in 400 µL of 4% formaldehyde (Fischer Scientific, cat#28906) for 20
183 minutes at room temperature, washed, and then permeabilized in equal volume of 0.1% saponin
184 (Sigma, cat#S4521) for 20 minutes. Alexa Fluor 488 Alkyne (Fisher Scientific, cat#A10267)
185 was used in place of Alexa Fluor 555 for FACS analysis.
186
187 **Flow cytometry**
188 Bone marrow cells were extracted by crushing bones from hind- and front limbs, hips, and
189 sternum, using mortar and pestle. Peritoneal cavity was isolated by flushing adult mice with 8
190 mL of FACS buffer (Hank's Balanced Salt Solution (Gibco, cat#14175-053) supplemented
191 with 0.5% Bovine Serum Albumin (Sigma, cat#A9647) and 2 mM EDTA (Invitrogen,
192 cat#15575-038)), or neonates 1-8 mL depending on the age. Red blood cell lysis was performed
193 on bone marrow and spleens using ACK lysis buffer (Fischer Scientific, cat#A1049201), only
194 for mice that were at least 19 days old. Lineage depletion was carried out before cell sorting by
195 MACS Cell Separation and LS columns (Miltenyi Biotec, cat#130-042-401) to deplete CD3+,
196 TER119+, or Gr-1+ cells, according to manufacturer's instructions.
197
198 Antibody staining of surface antigen was performed using FACS buffer, at a cell density of 1

199 x 10^7 cells per 100 µL of FACS buffer with antibodies, for 30 minutes at 4 ºC. Analysis of
200 intracellular antigens was done by using the same fixation and permeabilization as was
201 described under "Metabolic labeling of nascent proteins", or using BD Cytofix/Cytoperm
202 fixation/permeabilization kit (BD Biosciences, cat#554714). Maximum of 3 x 10^6 cells per
203 reaction. All flow cytometry experiments were gated on live CD19+ B cells and the following
204 immunophenotypes: Pro-B cells (CD93+IGM–cKIT+), Pre-B cells (CD93+IGM–cKIT– and
205 FSC-A to separate large from small), Imm-B cells (CD93+IGM+), peritoneal cavity B-1a B
206 cells (CD5+CD23–B220low and CD43+), and peritoneal cavity B-2 B cells (B220high CD23+
207 and CD43–). All flow cytometry experiments were performed at the Lund Stem Cell Center
208 FACS Core Facility (Lund University, Lund, Sweden) using BD Fortessa, BD Fortessa X20,
209 BD FACS Aria III, or BD FACS Aria II instruments. Cell sorting was performed using a 70
210 µm nozzle, 0.32.0 precision mask, and a flow rate below 6000 events/s. Analysis was
211 performed using FlowJo version 10. Antibodies are listed in Supplemental table S1.
212
213 **Bone marrow HSPC transplantation**
214 4000 bone marrow Lineage$^-$ Sca1$^+$ cKit$^+$ (LSK) donor cells (CD45.1) from day 10 neonatal
215 *Rpl24*$^{WT/Bst}$ or WT mice were FACS sorted and mixed at a 1:2 ratio with 8000 sorted CD45.1
216 competitor LSK cells and 200,000 CD45.1 total BM support cells. Cells were transplanted into
217 lethally irradiated (2 × 450 cGy) and CD45.1+ CD45.2+ double positive adult recipients by tail
218 vein injection. Endpoint analysis was performed 13–14 weeks after transplantation.
219
220 **In vivo treatment with Rapamycin**
221 Rapamycin (Enzo LifeSciences, cat#BML-A275-0005) was dissolved in Ethanol (99.5%,
222 Solveco, cat#11594139) and kept in -20 as stocks at a concentration of 10 mg/mL. Prior to
223 injection, stocks were further diluted in sterile DPBS (Cytiva, cat#SH30028.02) before
224 administering a single intraperitoneal injection of Rapamycin (2.5 mg/kg) or vehicle control
225 (36).
226
227 **Western Blot**
228 Sorted B cells were lysed in RIPA buffer (CST, cat#9806S), protease inhibitor (Roche,
229 cat#4693132001), and PMSF (CST, cat#8553S). Loading samples were prepared with
230 Laemmli buffer (Bio-Rad, cat#1610747) with β-mercaptoethanol (Bio-Rad, cat#1610710).
231 Proteins were separated by SDS–polyacrylamide gel electrophoresis (Any kD Mini-Protean
232 TGX gel, Bio-Rad, cat#4568125) and transferred to a nitrocellulose membrane (Trans-Blot
233 Turbo Mini Nitrocellulose Transfer Packs, Bio-Rad, cat#1704158). Membranes were blocked
234 for 1 hour at RT in 5% skimmed milk. Antibodies are listed in Supplemental table S1. The
235 ECL Select kit (GE Healthcare, cat#RPN2235) was used to detect protein bands with a
236 ChemiDoc XRS+ system (Bio-Rad).
237
238 For RIP validation western blot of Pro-B cells cultured ex vivo from bone marrow, 10% of the
239 total protein extract was collected to validate the immunoprecipitation efficiency. Proteins were
240 separated by SDS–polyacrylamide gel electrophoresis (12% Mini-Protean TGX gel, Bio-Rad,
241 cat#4561043) and transferred to a nitrocellulose membrane (Trans-Blot Turbo Mini

242 Nitrocellulose Transfer Packs, Bio-Rad, cat#1704158). Membranes were blocked for 1 hour at
243 RT in 5% skimmed milk. Antibodies are listed in Supplemental table S1.
244
245 **qRT-PCR**
246 50.000 sorted cells were lysed in RNAzol (Sigma-Aldrich, cat#R4533) and total RNA was
247 extracted using Direct-zol RNA MicroPrep kit (Zymo Research, cat#R2060) according to the
248 manufacturer's instructions. Total RNA (8 µl) was used in random primed cDNA synthesis
249 with TaqMan Reverse Transcription Reagents (Applied Biosystem, cat#N8080234). Diluted
250 cDNA 1:2 (4 µl) was used in every qPCR reaction using KAPA probe Fast qPCR kit (Kapa
251 Biosystem, cat#KK4706) with primers targeting 45S (Thermofisher Scientific, cat#
252 Mm03985792_s1) and 18S (Thermofisher Scientific, cat# 4333760T) rRNA transcripts. The
253 relative expression levels of rRNA were evaluated using log2 (2ΔCt) calculation.
254
255 **Statistical analysis**
256 All statistical analysis was carried out in R (version 4.1.2) and RStudio (version 1.4.1717),
257 using functions from the following packages: tidyverse (version 1.3.1), DESeq2 (version
258 1.32.0), rstatix (version 0.7.0), and ggpubr (version 0.4.0).

Results

The LIN28B mRNA interactome in primary B cell precursors is enriched for ribosomal protein transcripts

The developmentally restricted RNA binding protein LIN28B is a post-transcriptional regulator capable to regulating mRNA stability and translation. Using a tet-LIN28B inducible mouse model containing monoallelic expression of the *Col1a*$^{tetO\text{-}LIN28B}$ and *Rosa26*^{rtTA*m2} transgenes, we have previously demonstrated its ability to re-initiate fetal-like selection of B-1a cells in a cell intrinsic manner when ectopically expressed in hematopoietic progenitor cells(17, 19). To identify direct mRNA targets of LIN28B that could be important during B cell development, we took advantage of the FLAG tagged human LIN28B in the *Col1a*$^{tetO\text{-}LIN28B}$ allele of tet-LIN28B mice for immunoprecipitation of its mRNA interactome (33). To obtain sufficient cell numbers for interactome profiling, B cell precursors from uninduced tet-LIN28B and control mice were expanded for 5 days by culturing whole bone marrow cells in the presence of IL-7 and supplemented with Doxycycline (Dox) *ex vivo* to induce LIN28B expression. After five days with IL-7, the cultures reached above 80% B cell purity (Supplemental figure 1A). Cells were harvested and subjected to RNA immunoprecipitation (IP) coupled with poly-A selected RNA-sequencing (RIP-seq) (Figure 1A). Immunoprecipitation efficiency of LIN28B was validated by western blot analysis (Supplemental figure 1B). Total RNA sequencing of corresponding input samples was used for calculating RIP-seq enrichment. RIP/input ratio of the technical replicates showed a high degree of correlation ($R=0.93$, $p < 2.2e\text{-}16$) (Figure 1B) and were averaged for downstream analyses. 238 transcripts displayed a higher than two-fold RIP/input enrichment in tet-LIN28B samples but showed no trend in the control (Supplemental Table S2 and Figure 1C). Gene ontology (GO) analysis revealed a prominent enrichment for ribosomal protein coding transcripts (Figure 1D), suggesting that ribosomal function might be a core target pathway of LIN28B during B cell development. Interestingly, similar observations were previously made in other cell types, including 293T cells (22) and BE(2)-C neuroblastoma cells (31). Indeed, cross comparison of our identified targets with these studies yielded cytoplasmatic translation as the predominant overlapping GO term (Figure 1E-F). Our analysis also identified other GO terms involved in RNA splicing and oxidative phosphorylation, consistent with previous LIN28A/B interactome studies in various cell types (23, 37). We conclude that the direct LIN28B mRNA regulon in the context of primary bone marrow B cell progenitor cells is dominated by transcripts implicated in universal biosynthetic pathways, which are shared across a wide range of cell types. In particular, our findings implicate the ribosome as a potential target for LIN28B regulation in B cell progenitors.

LIN28B enhances protein synthesis in the small Pre-B and Imm-B stages of B cell development

LIN28B bound mRNA targets have been linked to both translational increase and decrease in a context dependent manner (22-31). In the case of ribosomal protein transcripts, enhanced protein translation has been shown by stable isotope labeling using amino acid in culture (22) as well as polysome profiling (31). To assess ribosomal protein levels during B cell

development, we performed western blot analysis on 50,000 sorted B cell precursors from tet-LIN28B and control mice following 10 days of Dox induction *in vivo* (Supplemental figure 2A). As expected, based on the dynamic changes in bioenergetic states during B cell development, the expression of ribosomal proteins rise and fall during the large and small Pre-B cells, respectively (Figure 2A). Consistent with enhanced translation, we found increased levels of ribosomal proteins upon LIN28B induction throughout B cell development.

Given this increase in ribosomal proteins, we expected a corresponding increase in ribosomal RNA (rRNA) content upon tet-LIN28B induction. To this end, we measured the 18S rRNAs by qRT-PCR of FACS sorted B cell precursors. In Pro and large-Pre-B cells, which are highly proliferative, we observed generally high rRNA content but no LIN28B dependent differences. rRNA content first began to increase in a LIN28B dependent manner in the quiescent small Pre-B cell stage and reached statistical significance in Imm-B cells (Figure 2B). Additional analysis of the 45S precursor rRNA showed the same trend (Figure 2C). Thus, the observed increase in ribosomal protein levels throughout B cell development (Figure 2A) does not exactly mirror the increase in ribosome biogenesis which is confined to the later stages of LIN28B induced B cell development. To evaluate whether this observation correlated with changes in global protein synthesis rates we measured newly synthesized proteins in freshly isolated B cell precursors using metabolic labelling with the methionine analog L-azidohomoalanine (AHA) (38). As expected, FACS readout of AHA uptake from Dox induced control and tet-LIN28B mice showed highly dynamic protein synthesis levels during B cell development (Figure 2D). Pro-B cells exhibited a bimodal profile with respect to protein synthesis that correlated with cell size (AHA^{high} or AHA^{low}, Supplemental figure 2B). Although there was a slight tendency towards more AHA^{high} Pro-B cells in tet-LIN28B induced mice, no statistical significance was detected in either the median fluorescence intensity (MFI) or frequency of the two subsets (Figure 2E, Supplemental figure 2C). Instead, LIN28B induced an increase in global protein synthesis in the small Pre-B and Imm-B cell stages. This result closely mirrors the observed effects on ribosome biogenesis (Figure 2B-C). Analysis of mature B cells showed that protein synthesis in peritoneal cavity B-1 and B-2 cells were not affected by LIN28B expression (Figure 2F), consistent with small Pre-B and Imm-B cells being uniquely sensitive to LIN28B induced changes in protein synthesis. Taken together, we conclude that LIN28B enhances ribosome content and global protein synthesis levels during the later stages of bone marrow B cell development.

IL-7 responsiveness dictates the stage specific effects of LIN28B during B cell development

Elevated ribosomal biogenesis is a hallmark of c-MYC activity (39). We have previously shown that LIN28B upregulates c-MYC protein levels in Imm-B cells (19). To investigate whether c-MYC up-regulation followed the observed LIN28B dependent effects on ribosome biogenesis and protein synthesis, we next analyzed c-MYC protein levels throughout B cell development using intracellular FACS. Consistent with its known IL-7 driven expression in Pro-B cells (2, 40), we found that c-MYC peaked in a subset of Pro-B cells regardless of genotype. The impact of LIN28B on c-MYC expression began in the small Pre-B cell stage and culminated in Imm-B cells (Figure 3A-B), mirroring the trend for ribosome biogenesis and

346 protein synthesis. This finding was consistent with changes at the transcriptome level, where
347 LIN28B induced a clear c-MYC target gene signature in the small Pre- and Imm-B cell stages
348 (Figure 3C). Interestingly, LIN28B induced de-repression of Let-7 targets was most apparent
349 during the IL-7 dependent Pro- and large Pre-B cell stages (Figure 3C) verifying the expected
350 effects of LIN28B action during early B cell development. Our results therefore indicate that a
351 shift in the LIN28B induced molecular program takes place during B cell development from a
352 largely c-MYC independent to a c-MYC dominated mode upon entry into quiescence in the
353 small Pre-B cell stage.
354
355 We next investigated the basis for the resistance to LIN28B induced effects on the c-MYC
356 /protein synthesis axis during the Pro- and large Pre-B cell stages. Here, IL-7 is a major trophic
357 factor driving c-MYC expression prior to the Pre-BCR checkpoint (2, 40). We therefore
358 hypothesized that IL-7 signaling might mask any LIN28B mediated effects on c-MYC. To test
359 this, we expanded B cell precursors from control and tet-LIN28B bone marrow under saturating
360 IL-7 conditions for five days, before replating the cells under limiting doses of IL-7 (Figure
361 3D) as previously described (Mandal 2019). Two days following IL-7 withdrawal, cultured
362 cells were harvested and FACS analyzed for LIN28B-dependent effects on c-MYC expression
363 and global protein synthesis in Pro-B cells. As expected, IL-7 withdrawal resulted in to a dose
364 dependent decrease in c-MYC and a collapse in the protein synthesis of Pro-B cells (Figure
365 3E-F). Interestingly, the observed decrease in c-MYC was partially alleviated by tet-LIN28B
366 induction *ex vivo* at limiting IL-7 conditions (Figure 3E left). A similar trend was observed for
367 protein synthesis (Figure 3E right). Taken together, we demonstrate that LIN28B exerts an
368 upregulation of the c-MYC/protein synthesis axis during B cell development. During the Pro-
369 and Pre-B cell stages, the LIN28B effect is normally masked by IL-7 signaling and is only
370 revealed upon acute IL-7 withdrawal. In contrast, c-Myc is consistently sensitive to LIN28B in
371 small Pre-B and Imm-B cells which are not responsive to IL-7. These findings provide an
372 explanation to the observed stage specific effects on the c-MYC/protein synthesis axis exerted
373 by LIN28B during B cell development (Figure 3F).
374
375 **Neonatal B cell development relies on a heightened level of protein synthesis**
376 Endogenous LIN28B expression is developmentally limited to fetal and neonatal life. FACS
377 analysis of LIN28B-eGFP reporter mice (34) captured its window of expression in B cell
378 precursors as it gradually diminished to background levels after day 10 (Figure 4A). During
379 the same window, protein synthesis in wildtype neonatal bone marrow small Pre-B and Imm-
380 B cells was also elevated (Figure 4B). This effect was LIN28B dependent and fully abolished
381 in 3-day-old neonates that lacked endogenous *Lin28b* (Figure 4C). In contrast, *Lin28b*
382 deficiency did not affect protein synthesis in neonatal Pro-B cells. These findings confirm our
383 results from tet-LIN28B induction in adulthood and establish increased protein synthesis by
384 endogenous *Lin28b* as a hallmark of early life B cell development in wildtype mice.
385
386 To investigate the importance of elevated protein synthesis for neonatal B cell development,
387 we took advantage of the ribosomal protein hypomorphic *Rpl24*$^{WT/Bst}$ mouse model. This model
388 carries a mutation that disrupts *Rpl24* mRNA splicing and thereby ribosome biogenesis,
389 exhibiting a 30% reduction in overall protein synthesis (41). This reduction does not affect

390 steady-state adult B lymphopoiesis (38), but is sufficient to impair Eμ-MYC driven
391 oncogenesis (42). Given our findings in neonates and tet-LIN28B mice, we hypothesized that
392 early-life B lymphopoiesis would be more sensitive to the constraints in protein synthesis
393 imposed by the Bst mutation (Figure 4D). Indeed, analysis of *Rpl24*$^{WT/Bst}$ bone marrow revealed
394 decreased overall B cell frequency on postnatal day three and ten (Figure 4E). Thus, a
395 heightened sensitivity to constrained protein synthesis in the B cell lineage coincided with the
396 time window for endogenous *Lin28b* expression. Reduced bone marrow B cell frequency
397 reflected a decrease in B cell precursors during this window, which was fully resolved by day
398 19 (Figure 4F). This defect translated into a decrease in the frequency of both CD5+ B-1a and
399 B-2 cells early in life, consistent with a reduction in the overall quantitative output of B cells
400 in neonatal *Rpl24*$^{WT/Bst}$ mice (Figure 4G). To verify that these observed effects were cell
401 intrinsic, we performed competitive transplantations of neonatal *Rpl24*$^{WT/Bst}$ or wildtype
402 littermate bone marrow hematopoietic stem and progenitor cells (HSPCs) into lethally
403 irradiated hosts (Figure 4H). Analysis of host peritoneal cavity at 14 weeks post-transplantation
404 showed a selective decrease in B-1a cell reconstitution from *Rpl24*$^{WT/Bst}$ donor cells. In contrast,
405 contribution to the B-2 compartment, that is continuously replenished by adult B
406 lymphopoiesis, was comparable between the *Rpl24*$^{WT/Bst}$ and wildtype donor HSPCs (Figure
407 4I). Taken together, these findings demonstrate that neonatal B lymphopoiesis in a cell intrinsic
408 manner exhibits heightened sensitivity to constraints in protein synthesis compared to the adult.
409
410 **Elevated protein synthesis is required for the output of self-reactive B-1a cells early in life**
411 The early-life expression of *Lin28b* allows for the developmental progression of self-reactive
412 B cell precursors into the mature B cell pool, including the output of CD5+ B-1a cells (19, 20).
413 This relaxation of central tolerance is evident in recently selected Imm-B cells where LIN28B
414 expression increases surface levels of CD5, a marker for self-reactivity (19). Interestingly,
415 analysis of tet-LIN28B induced Imm-B cells revealed that CD5 expression positively
416 correlated with protein synthesis levels (Figure 5A-B). Thus, enhanced protein synthesis may
417 be particularly important for the developmental progression of self-reactive B cells destined
418 for the CD5+ B-1a cell fate. To test this, we treated tet-LIN28B induced mice with a single
419 dose of intraperitoneally administered Rapamycin to acutely dampen protein synthesis (Figure
420 5C) (43). As expected, the treatment yielded a moderate reduction in protein synthesis levels
421 in both control and tet-LIN28B Imm-B cells, reducing the tet-LIN28B Imm-B cells to untreated
422 wildtype levels of protein synthesis (Figure 5D). Interestingly, this treatment selectively
423 diminished the CD5 levels in tet-LIN28B induced Imm-B cells (Figure 5E-F). We conclude
424 that LIN28B dependent output of self-reactive B cells depends on increased protein synthesis.
425
426 Finally, to investigate the qualitative impact of constrained protein synthesis on early life B
427 cell output, we measured the abundance of the known ontogenically restricted B-1 cell
428 specificity against the self-membrane component phosphatidyl choline (PtC) in 19-day-old Bst
429 mice. This timepoint was selected to evaluate PtC+ B-1 cell output with minimal influence by
430 peripheral homeostatic expansion (44). Indeed, FACS analysis using PtC liposomes revealed
431 a three-fold decrease of reactive B cells in the peritoneal cavity of *Rpl24*$^{WT/Bst}$ mice (Figure 5G-
432 H). We therefore conclude that elevated protein synthesis is a central distinguishing parameter

433 of overall neonatal B lymphopoiesis that potentiates the output of CD5+ B-1 cells with self-
434 reactive BCR specificities.

435 **Discussion**
436 Our findings identified elevated protein synthesis as a hallmark of neonatal B cell development
437 that was required for overall B cell output early in life including the time restricted output of
438 self-reactive B-1 cells. This was mediated in part by the endogenous expression of the
439 heterochronic RNA-binding protein LIN28B. Its expression naturally waned during the first
440 weeks of life and ectopic LIN28B expression was sufficient to recapitulate elevated protein
441 synthesis in adult small Pre- and Imm-B cells. Consistent with previous reports, we showed
442 that LIN28B directly bound to ribosomal protein transcripts and correlated with enhanced
443 ribosomal protein expression in primary B cell precursors. Interestingly, an increase in
444 ribosomal biogenesis and protein synthesis coincided with LIN28B induced c-MYC expression
445 in the quiescent small Pre- and Imm-B cell stages. The precise extent and mechanism by which
446 LIN28B post-transcriptionally cooperates with a c-MYC induced transcriptome was not
447 disentangled in this study. Nevertheless, our findings implicate ribosomal regulation in the
448 control of neonatal B cell development with important implications in the layered formation of
449 the immune system.
450
451 Protein synthesis is the most energy consuming biosynthetic process in the cell and subject to
452 the constraints imposed by hundreds of components required for ribosome assembly (45).
453 Indeed, protein synthesis rates give an accurate account of the overall cellular metabolism (46).
454 And yet, its ability to control the development and function of immune cells that require rapid
455 expansion and contraction of cellular growth has been an under-explored subject of
456 investigation. Our results using AHA metabolic labelling to measure protein synthesis
457 confirmed dynamic changes in cellular metabolism that underly proliferative bursts following
458 successful BCR checkpoints (1). Importantly, we demonstrated the ability of LIN28B to
459 partially alleviate the biggest drop in protein synthesis upon entry into the small Pre-B cell
460 stage. The restricted metabolism of small Pre-B cells was previously implicated as a
461 mechanism to safeguard the central tolerance checkpoint through enforcing nutrient stress and
462 negative selection upon strong BCR engagement (5). This notion is highly compatible with our
463 observation that LIN28B promoted protein synthesis to augment the output of self-reactive
464 CD5+ B-1 cells early in life. Thus, we propose that the relatively mild increase in protein
465 synthesis mediated by LIN28B provides sufficient relaxation of the metabolic constraints
466 during B cell maturation to qualitatively alter the B cell output.
467
468 In Pro-B cells, IL-7 signaling and downstream mTORC1 activation is the principal driver of c-
469 MYC expression and acts to promote biomass accumulation and proliferation (Zeng et al
470 2018). In this study, we showed that the attenuation of IL-7 signaling during B cell
471 development correlated with distinct outcomes of LIN28B mediated effects. While de-
472 repression of Let-7 targets was most prominent during the IL-7 dependent stages, the effect on
473 protein synthesis instead appeared later during the IL-7 independent stages. This could be due
474 to changes in the abundance of LIN28B/Let-7 RNA substrates in proliferating versus quiescent
475 cells respectively. Therefore, our findings implicate metabolic status as a powerful rheostat of
476 LIN28B action. Interestingly, IL-7 withdrawal of Pro-B cells *ex vivo* mimicked the situation
477 during the later IL-7 independent, small Pre-B and Imm-B cell, stages revealing a LIN28B
478 mediated effect on c-MYC and protein synthesis. This finding is consistent with the ability of

479 LIN28B to mitigate the strict requirement for IL-7Ra during adult B lymphopoiesis (16). Thus,
480 overlapping but milder effects by LIN28B on the same c-MYC/protein synthesis axis may offer
481 an explanation to the lessened reliance on IL-7 for early life B lymphopoiesis (6).
482
483 In this study we did not resolve the fates of LIN28B bound transcripts in the rapidly alternating
484 stages of B cell development. One obstacle preventing the examination of the context
485 dependent, direct effects of LIN28B is the limited cellular material from quiescent cell types
486 *in vivo*, particularly from neonates. Methods such as polysome sequencing to profile changes
487 in protein translation are optimized for proliferating cells and require a sizable cell pool.
488 However, our findings suggest that artificial increases in cellular metabolism by *in vitro*
489 culturing or oncogene mediated transformation might obscure any physiological LIN28B
490 mediated effects. Despite this limitation, our results demonstrate that protein synthesis is an
491 important differentially regulated feature of neonatal B lymphopoiesis and open new avenues
492 for future investigations. In the context of B cell neoplasms, protein synthesis is a key mediator
493 of c-MYC driven oncogenesis (42). Considering the strong infant and childhood association of
494 B cell precursor acute lymphoblastic leukemia incidence, it will be important to investigate a
495 potential role for increased ribosome addiction in the pathogenesis of the disease. In the context
496 of neonatal immunity, we and others have previously demonstrated that neonatal antigen
497 exposure produces unique B cell memory clones not generated by adult mice immunized with
498 the same antigen (47, 48). Our current findings that enhanced protein synthesis quantitatively
499 and qualitatively alters neonatal B cell output implicates ribosomal control in the formation of
500 a layered immune system.

Acknowledgements

We thank Jonas Ungerbäck and Johanna Tingvall-Gustafsson for help with bioinformatics. We thank Jenny Hansson, Leal Oburoglu, and Svetlana Soboleva for their input. Finally, we also thank the FACS and Bioinformatics core facilities at the Lund Stem Cell Center for their support.

Funding

J.Y. was supported by the Swedish Research Council, the Swedish Cancer Society, the European Research Council (715313), Knut and Alice Wallenberg Foundation and the Wenner-Gren Foundations.

510 **References**

511 1. Clark MR, Mandal M, Ochiai K, Singh H. Orchestrating B cell lymphopoiesis through interplay of
512 IL-7 receptor and pre-B cell receptor signalling. Nat Rev Immunol. 2014;14(2):69-80.
513 2. Zeng H, Yu M, Tan H, Li Y, Su W, Shi H, et al. Discrete roles and bifurcation of PTEN signaling and
514 mTORC1-mediated anabolic metabolism underlie IL-7-driven B lymphopoiesis. Sci Adv.
515 2018;4(1):eaar5701.
516 3. Mandal M, Okoreeh MK, Kennedy DE, Maienschein-Cline M, Ai J, McLean KC, et al. CXCR4
517 signaling directs Igk recombination and the molecular mechanisms of late B lymphopoiesis. Nat
518 Immunol. 2019;20(10):1393-403.
519 4. Nemazee D. Mechanisms of central tolerance for B cells. Nat Rev Immunol. 2017;17(5):281-94.
520 5. Muschen M. Metabolic gatekeepers to safeguard against autoimmunity and oncogenic B cell
521 transformation. Nat Rev Immunol. 2019;19(5):337-48.
522 6. Kikuchi K, Kondo M. Developmental switch of mouse hematopoietic stem cells from fetal to
523 adult type occurs in bone marrow after birth. Proc Natl Acad Sci U S A. 2006;103(47):17852-7.
524 7. Hayakawa K, Asano M, Shinton SA, Gui M, Allman D, Stewart CL, et al. Positive selection of
525 natural autoreactive B cells. Science. 1999;285(5424):113-6.
526 8. Chen JW, Rice TA, Bannock JM, Bielecka AA, Strauss JD, Catanzaro JR, et al. Autoreactivity in
527 naive human fetal B cells is associated with commensal bacteria recognition. Science.
528 2020;369(6501):320-5.
529 9. Wong JB, Hewitt SL, Heltemes-Harris LM, Mandal M, Johnson K, Rajewsky K, et al. B-1a cells
530 acquire their unique characteristics by bypassing the pre-BCR selection stage. Nat Commun.
531 2019;10(1):4768.
532 10. Baumgarth N. The double life of a B-1 cell: self-reactivity selects for protective effector
533 functions. Nat Rev Immunol. 2011;11(1):34-46.
534 11. Ambros V, Horvitz HR. Heterochronic mutants of the nematode Caenorhabditis elegans.
535 Science. 1984;226(4673):409-16.
536 12. Copley MR, Eaves CJ. Developmental changes in hematopoietic stem cell properties. Exp Mol
537 Med. 2013;45:e55.
538 13. Zhou Y, Li YS, Bandi SR, Tang L, Shinton SA, Hayakawa K, et al. Lin28b promotes fetal B
539 lymphopoiesis through the transcription factor Arid3a. J Exp Med. 2015;212(4):569-80.
540 14. Copley MR, Babovic S, Benz C, Knapp DJ, Beer PA, Kent DG, et al. The Lin28b-let-7-Hmga2 axis
541 determines the higher self-renewal potential of fetal haematopoietic stem cells. Nat Cell Biol.
542 2013;15(8):916-25.
543 15. Sampson VB, Rong NH, Han J, Yang Q, Aris V, Soteropoulos P, et al. MicroRNA let-7a down-
544 regulates MYC and reverts MYC-induced growth in Burkitt lymphoma cells. Cancer Res.
545 2007;67(20):9762-70.
546 16. Yuan J, Nguyen CK, Liu X, Kanellopoulou C, Muljo SA. Lin28b reprograms adult bone marrow
547 hematopoietic progenitors to mediate fetal-like lymphopoiesis. Science. 2012;335(6073):1195-
548 200.
549 17. Kristiansen TA, Jaensson Gyllenback E, Zriwil A, Bjorklund T, Daniel JA, Sitnicka E, et al. Cellular
550 Barcoding Links B-1a B Cell Potential to a Fetal Hematopoietic Stem Cell State at the Single-Cell
551 Level. Immunity. 2016;45(2):346-57.
552 18. Wang J, Wissink EM, Watson NB, Smith NL, Grimson A, Rudd BD. Fetal and adult progenitors
553 give rise to unique populations of CD8+ T cells. Blood. 2016;128(26):3073-82.

554 19. Vanhee S, Akerstrand H, Kristiansen TA, Datta S, Montano G, Vergani S, et al. Lin28b controls a
555 neonatal to adult switch in B cell positive selection. Sci Immunol. 2019;4(39).
556 20. Xu X, Deobagkar-Lele M, Bull KR, Crockford TL, Mead AJ, Cribbs AP, et al. An ontogenetic switch
557 drives the positive and negative selection of B cells. Proc Natl Acad Sci U S A. 2020;117(7):3718-
558 27.
559 21. Benhamou D, Labi V, Novak R, Dai I, Shafir-Alon S, Weiss A, et al. A c-Myc/miR17-92/Pten Axis
560 Controls PI3K-Mediated Positive and Negative Selection in B Cell Development and
561 Reconstitutes CD19 Deficiency. Cell Rep. 2016;16(2):419-31.
562 22. Graf R, Munschauer M, Mastrobuoni G, Mayr F, Heinemann U, Kempa S, et al. Identification of
563 LIN28B-bound mRNAs reveals features of target recognition and regulation. RNA Biol.
564 2013;10(7):1146-59.
565 23. Wilbert ML, Huelga SC, Kapeli K, Stark TJ, Liang TY, Chen SX, et al. LIN28 binds messenger RNAs
566 at GGAGA motifs and regulates splicing factor abundance. Mol Cell. 2012;48(2):195-206.
567 24. Cho J, Chang H, Kwon SC, Kim B, Kim Y, Choe J, et al. LIN28A is a suppressor of ER-associated
568 translation in embryonic stem cells. Cell. 2012;151(4):765-77.
569 25. Hafner M, Max KE, Bandaru P, Morozov P, Gerstberger S, Brown M, et al. Identification of
570 mRNAs bound and regulated by human LIN28 proteins and molecular requirements for RNA
571 recognition. RNA. 2013;19(5):613-26.
572 26. Wang S, Chim B, Su Y, Khil P, Wong M, Wang X, et al. Enhancement of LIN28B-induced
573 hematopoietic reprogramming by IGF2BP3. Genes Dev. 2019;33(15-16):1048-68.
574 27. Basak A, Munschauer M, Lareau CA, Montbleau KE, Ulirsch JC, Hartigan CR, et al. Control of
575 human hemoglobin switching by LIN28B-mediated regulation of BCL11A translation. Nat Genet.
576 2020;52(2):138-45.
577 28. Osborne JK, Kinney MA, Han A, Akinnola KE, Yermalovich AV, Vo LT, et al. Lin28 paralogs
578 regulate lung branching morphogenesis. Cell Rep. 2021;36(3):109408.
579 29. Madison BB, Liu Q, Zhong X, Hahn CM, Lin N, Emmett MJ, et al. LIN28B promotes growth and
580 tumorigenesis of the intestinal epithelium via Let-7. Genes Dev. 2013;27(20):2233-45.
581 30. Tan FE, Sathe S, Wheeler EC, Yeo GW. Non-microRNA binding competitively inhibits LIN28
582 regulation. Cell Rep. 2021;36(6):109517.
583 31. Missios P, da Rocha EL, Pearson DS, Philipp J, Aleman MM, Pirouz M, et al. LIN28B alters
584 ribosomal dynamics to promote metastasis in MYCN-driven malignancy. J Clin Invest.
585 2021;131(22).
586 32. Peng S, Chen LL, Lei XX, Yang L, Lin H, Carmichael GG, et al. Genome-wide studies reveal that
587 Lin28 enhances the translation of genes important for growth and survival of human embryonic
588 stem cells. Stem Cells. 2011;29(3):496-504.
589 33. Zhu H, Shyh-Chang N, Segre AV, Shinoda G, Shah SP, Einhorn WS, et al. The Lin28/let-7 axis
590 regulates glucose metabolism. Cell. 2011;147(1):81-94.
591 34. Kristiansen TA, Zhang Q, Vergani S, Boldrin E, Krausse N, Andre O, et al. Developmental cues
592 license megakaryocyte priming in murine hematopoietic stem cells. Blood Adv. 2022.
593 35. Holl TM, Haynes BF, Kelsoe G. Stromal cell independent B cell development in vitro: generation
594 and recovery of autoreactive clones. J Immunol Methods. 2010;354(1-2):53-67.
595 36. Ersching J, Efeyan A, Mesin L, Jacobsen JT, Pasqual G, Grabiner BC, et al. Germinal Center
596 Selection and Affinity Maturation Require Dynamic Regulation of mTORC1 Kinase. Immunity.
597 2017;46(6):1045-58 e6.

598 37. Shyh-Chang N, Zhu H, Yvanka de Soysa T, Shinoda G, Seligson MT, Tsanov KM, et al. Lin28
599 enhances tissue repair by reprogramming cellular metabolism. Cell. 2013;155(4):778-92.
600 38. Signer RA, Magee JA, Salic A, Morrison SJ. Haematopoietic stem cells require a highly regulated
601 protein synthesis rate. Nature. 2014;509(7498):49-54.
602 39. Ruggero D. The role of Myc-induced protein synthesis in cancer. Cancer Res. 2009;69(23):8839-
603 43.
604 40. Morrow MA, Lee G, Gillis S, Yancopoulos GD, Alt FW. Interleukin-7 induces N-myc and c-myc
605 expression in normal precursor B lymphocytes. Genes Dev. 1992;6(1):61-70.
606 41. Oliver ER, Saunders TL, Tarle SA, Glaser T. Ribosomal protein L24 defect in belly spot and tail
607 (Bst), a mouse Minute. Development. 2004;131(16):3907-20.
608 42. Barna M, Pusic A, Zollo O, Costa M, Kondrashov N, Rego E, et al. Suppression of Myc oncogenic
609 activity by ribosomal protein haploinsufficiency. Nature. 2008;456(7224):971-5.
610 43. Beretta L, Gingras AC, Svitkin YV, Hall MN, Sonenberg N. Rapamycin blocks the phosphorylation
611 of 4E-BP1 and inhibits cap-dependent initiation of translation. EMBO J. 1996;15(3):658-64.
612 44. Yang Y, Wang C, Yang Q, Kantor AB, Chu H, Ghosn EE, et al. Distinct mechanisms define murine
613 B cell lineage immunoglobulin heavy chain (IgH) repertoires. Elife. 2015;4:e09083.
614 45. Buttgereit F, Brand MD. A hierarchy of ATP-consuming processes in mammalian cells. Biochem
615 J. 1995;312 (Pt 1):163-7.
616 46. Arguello RJ, Combes AJ, Char R, Gigan JP, Baaziz AI, Bousiquot E, et al. SCENITH: A Flow
617 Cytometry-Based Method to Functionally Profile Energy Metabolism with Single-Cell Resolution.
618 Cell Metab. 2020;32(6):1063-75 e7.
619 47. Vergani S, Muleta KG, Da Silva C, Doyle A, Kristiansen TA, Sodini S, et al. A self-sustaining layer
620 of early-life-origin B cells drives steady-state IgA responses in the adult gut. Immunity. 2022.
621 48. New JS, Dizon BLP, Fucile CF, Rosenberg AF, Kearney JF, King RG. Neonatal Exposure to
622 Commensal-Bacteria-Derived Antigens Directs Polysaccharide-Specific B-1 B Cell Repertoire
623 Development. Immunity. 2020;53(1):172-86 e6.

624

625

Table S1. Antibodies and reagents used for Flow Cytometry, Western Blot, or IP

Antigen	Fluorochrome	Clone	Manufacturer	Reference#
7-AAD	-	-	BD Bioscience	559925
B220	APC Cy7	RA3-6B2	BioLegend	103224
B220	PE CF594	RA3-6B2	BD Biosciences	562313
CD117	BV421	2B8	BD Biosciences	562609
CD117	PE	2B8	Invitrogen	12-1171-82
CD19	APC Cy7	1D3	BD Biosciences	557655
CD19	BV786	1D3	BD Biosciences	563333
CD23	PE Cy7	B3B4	BioLegend	101614
CD25	PE eFluor610	PC61.5	Invitrogen	61-0251-82
CD3	PE Cy5	145-2C11	BioLegend	100310
CD43	FITC	S7	BD Biosciences	553270
CD5	BV421	53-3.3	BD Biosciences	562739
CD5	PE	53-7.3	BioLegend	100608
CD93	APC	AA4.1	BioLegend	136510
CD93	BV786	AA4.1	BD Biosciences	740941
c-MYC	Unconjugated	Y69	Abcam	Ab32072
Goat anti-Rabbit IgG (H+L) Cross-Adsorbed Secondary Antibody	AF647	Polyclonal	Invitrogen	A-21244
Gr-1	PE Cy5	RB6-8C5	BioLegend	108410
IgM	FITC	11/41	BD Biosciences	553437
IgM	PE Cy7	RMM-1	BioLegend	406514
Alkyne, 5-isomer	AF488	-	Invitrogen	A10267
PtC	Marina Blue	DOPC/CHOL Liposomes	Formumax	F60103F-MB
Ter119	PE Cy5	TER-119	BioLegend	116210
Tubulin alpha			CST	2125
RPL23			Abcam	ab264369
RPL36a			Invitrogen	PA5-70719
RPS9			Abcam	ab157125
FLAG M2			Sigma	F1804
LIN28B			CST	4196

629 **Captions**
630
631 **Figure 1. LIN28B binds to ribosomal protein transcripts in primary B cell precursors**
632
633 **(A)** Schematic of experimental setup for the identification of LIN28B-mRNA targets in bone
634 marrow (BM) B cell precursors. Uninduced total BM cells were expanded for Pro-B cells in
635 the presence of IL-7 (20 ng/mL) and Doxycycline (Dox, 0.1 µg/mL) for five days prior to
636 RNA-IP. Co-immunoprecipitated mRNA from two tet-LIN28B and one control mouse were
637 individually subjected to Poly-A RNA-seq and enrichment over input RNA was determined.
638 **(B)** IP/input enrichment ratios from the two tet-LIN28B samples were plotted against each
639 other showing high correlation between the two biological replicates. LIN28B IP/input
640 enrichment ratio of least two-fold (n=238 transcripts) were used for subsequent analyses. **(C)**
641 Average enrichment ratio ranking of the tet-LIN28B samples compared to the control sample.
642 **(D)** Top ten gene ontology terms of the 238 enriched transcripts. **(E)** Analysis of overlapping
643 genes between the 238 LIN28B enriched transcripts (Åkerstrand et al) and previously
644 published LIN28B-mRNA interactome data sets (22, 31). **(F)** Gene ontology analyses of
645 overlapping LIN28B enriched transcripts between the indicated study and the 238 transcripts.
646

647 **Figure 2. LIN28B enhances ribosome biogenesis and protein synthesis in small Pre-B and**
648 **Imm-B cells**
649
650 **(A)** Western blot analysis for the indicated ribosomal proteins from 50,000 FACS sorted B cell
651 progenitors from tet-LIN28B or littermate control mice following 10 days of *in vivo* Dox
652 induction. Representative of at least two biological replicates per cell type and genotype. **(B-**
653 **C)** qRT-PCR for 18S rRNA or 45S pre-rRNA from 50,000 FACS sorted B cell progenitors.
654 Expression values were normalized relative to the littermate control Imm-B cells. Large and
655 small Pre-B cells are indicated as Lg and Sm respectively. **(D)** Representative FACS histogram
656 overlays of L-Azidohomoalanine (AHA) uptake, corresponding to their protein synthesis rates,
657 in the indicated subsets. **(E)** Average AHA median fluorescence intensity (MFI) for indicated
658 bone marrow B cell progenitor stage, after normalization to the littermate control small Pre-B
659 MFI. **(F)** Average AHA MFI for the indicated, mature peritoneal cavity (PerC) B cells, plotted
660 relative to the control B-2 values on a Log2 scale. Wilcox test was used to calculate p-values.
661 *p<0.05, **p<0.01, ***p<0.001. Error bars show standard deviation.
662

663 **Figure 3. IL-7 signaling masks the effects of LIN28B on the c-MYC / protein synthesis**
664 **axis in Pro-B cells**
665
666 **(A)** Representative histograms showing intracellular FACS analysis of c-MYC protein
667 expression in the indicated populations from littermate control or tet-Lin28b mouse. **(B)**
668 Average c-MYC MFI for indicated subsets shown as relative values to the control small Pre-B
669 cell population. **(C)** Gene set enrichment analysis (GSEA) of differentially expressed genes
670 between tet-LIN28B induced and control B cell precursor subsets as identified by RNAseq
671 (See methods). Vertical line indicates Zero cross point. **(D)** Experimental setup for measuring

672 the impact of IL-7 availability on sensitivity to LIN28B mediated effects on Pro-B cells.
673 Following 5 days of expanding B cell precursors in 20 ng/mL IL-7, the culture were split into
674 conditions with decreasing concentrations of IL-7. Two days later, the cultures were analyzed
675 by FACS for intracellular c-MYC and AHA uptake. **(E)** Representative FACS histograms for
676 the indicated IL-7 conditions show c-MYC protein expression (left) and AHA uptake (right) in
677 Pro-B cells. **(F)** Schematic illustration of the proposed LIN28B impact on protein synthesis in
678 B cell precursors in the presence or absence of IL-7 signaling. Wilcox test was used to calculate
679 p-values in B. **p<0.01, ***p<0.001. Error bars show standard deviation.
680
681 **Figure 4. Neonatal B cell development is dependent on enhanced protein synthesis**
682 **(A)** Analysis of BM B cell precursors from *Lin28b*-eGFP mice at the indicated ages. The
683 average frequency of *Lin28b*-eGFP positive cells is shown for each day. **(B)** Average AHA
684 MFI are plotted relative to the adult control for each experiment. **(C)** Average AHA MFI in 3-
685 day old WT or *Lin28b* KO neonates. Values are displayed relative to small Pre-B cells from
686 *Lin28b* KO neonates in each experiment. **(D)** Experimental overview for investigating age-
687 specific defect under limited protein synthesis rates. *Rpl24*$^{wt/Bst}$ and wildtype littermate controls
688 were analyzed by FACS at different ages for phenotypic BM B cell development. **(E)** Average
689 CD19+ B cell frequencies out of total BM cells at the indicated ages. **(F)** Average BM B cell
690 precursor subset frequencies at the indicated ages presented as frequency of total BM cells. **(G)**
691 Average mature PerC B-1a and B-2 cell frequencies out of total PerC cells in *Rpl24*$^{wt/Bst}$ or WT
692 littermate control mice at the indicated ages. **(H)** Experimental overview for assessment of cell
693 intrinsic defect of the Bst mutation. Lineage–, Sca1+, cKit+ (LSK) hematopoietic stem and
694 progenitor cells (HSPCs) from 10-day-old donor and competitor mice of the indicated
695 genotypes were sorted and transplanted into lethally irradiated recipients. 13-14 weeks later,
696 the steady state donor and competitor derived mature PerC B cells were compared to assess B-
697 1a and B-2 cell output. **(I)** CD19+ PerC B cells of the indicated subtypes were compared for
698 donor versus competitor contribution. Average frequencies are displayed. T-test was used to
699 calculate p-values *p<0.05, **p<0.01, ***p<0.001. Error bars show standard deviation.
700
701 **Figure 5. Elevated protein synthesis is required for the output of CD5+ B-1 cells early in**
702 **life**
703 **(A)** (Left) Representative FACS plots for CD5 expression in Imm-B cells from the indicated
704 genotypes (left) and corresponding AHA uptake of the indicated subsets (right). **(B)** Average
705 AHA MFI within individual CD5 slices, after normalization to AHA MFI in littermate
706 control Imm-B cells. **(C)** Schematic for treatment of tet-LIN28B and littermate control mice
707 with Rapamycin (Rapa, 2 mg/kg), or vehicle control (EtOH). Mice were given a single, intra-
708 peritoneal injection and analyzed 24hrs later. **(D)** AHA MFI from Imm-B cells of the
709 indicated genotype and treatment. MFI was normalized to EtOH treated littermate control
710 Imm-B cells. **(E)** Representative FACS histograms show Imm-B CD5 levels following the
711 indicated treatment. **(F)** Summary of data shown in E. Data is normalized to EtOH treated
712 littermate controls within each experiment and averaged between biological replicates. **(G)**
713 Representative FACS plots showing the frequency of CD5+ PtC reactive B cells in 19-day
714 old wildtype littermate control or Rpl24$^{wt/Bst}$ neonates. **(H)** Average CD5+PtC+ frequency out

715 of PerC CD19+ B cells in 19-day old mice. Wilcox test was used to calculate p-values
716 *$p<0.05$, **$p<0.01$. Error bars show standard deviation.

Figure 1

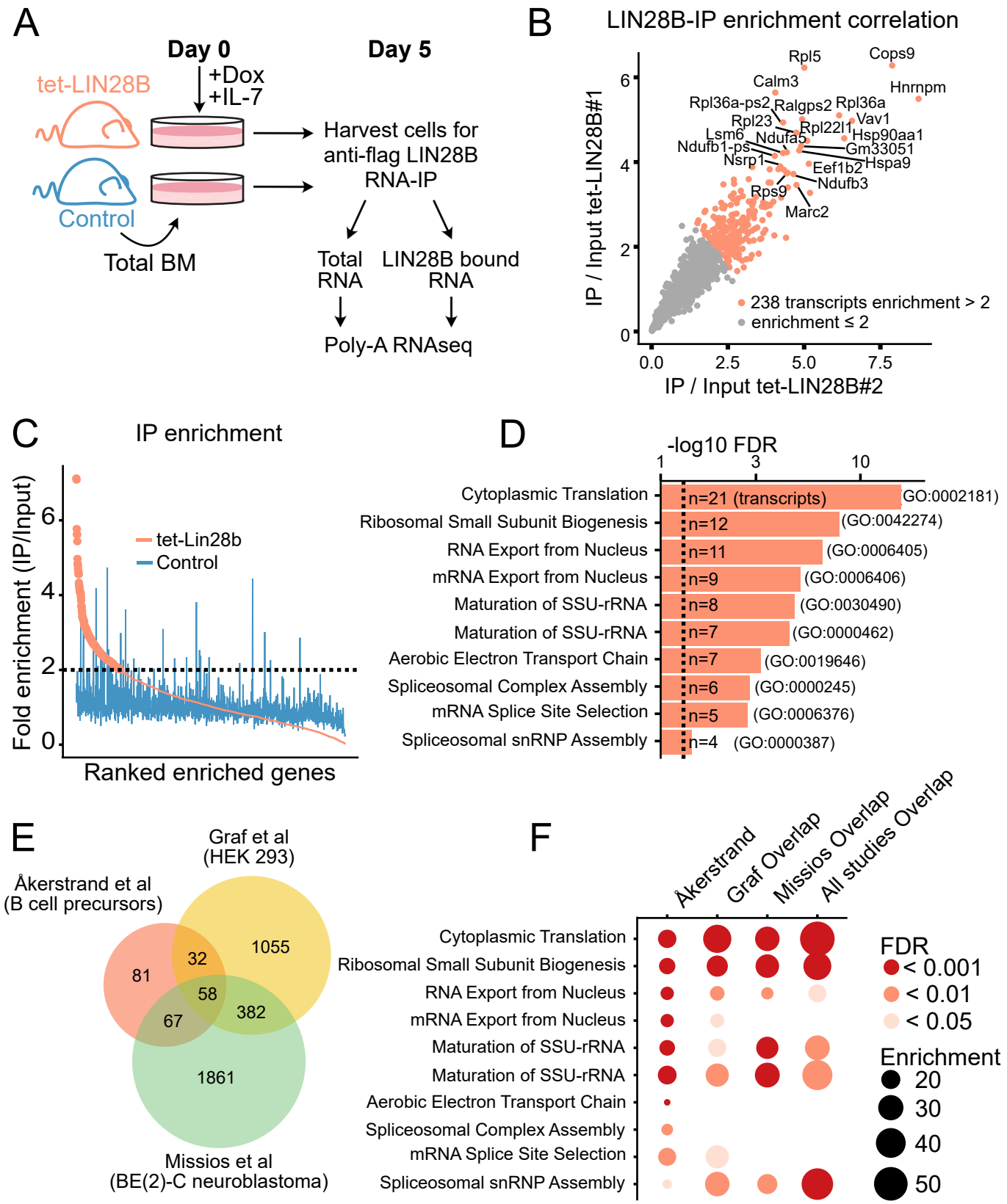
A
Day 0
Day 5
tet-LIN28B
+Dox
+IL-7
Harvest cells for
anti-flag LIN28B
RNA-IP
Control
Total BM
Total
RNA
LIN28B bound
RNA
Poly-A RNAseq
B
LIN28B-IP enrichment correlation
IP / Input tet-LIN28B#1
IP / Input tet-LIN28B#2
Rpl5
Cops9
Calm3
Hnrnpm
Rpl36a-ps2
Ralgps2
Rpl36a
Rpl23
Vav1
Rpl22l1
Lsm6
Ndufa5
Hsp90aa1
Ndufb1-ps
Gm33051
Nsrp1
Eef1b2
Hspa9
Ndufb3
Rps9
Marc2
238 transcripts enrichment > 2
enrichment ≤ 2
C
IP enrichment
Fold enrichment (IP/Input)
tet-Lin28b
Control
Ranked enriched genes
D
-log10 FDR
Cytoplasmic Translation
n=21 (transcripts)
GO:0002181)
Ribosomal Small Subunit Biogenesis
n=12
(GO:0042274)
RNA Export from Nucleus
n=11
(GO:0006405)
mRNA Export from Nucleus
n=9
(GO:0006406)
Maturation of SSU-rRNA
n=8
(GO:0030490)
Maturation of SSU-rRNA
n=7
(GO:0000462)
Aerobic Electron Transport Chain
n=7
(GO:0019646)
Spliceosomal Complex Assembly
n=6
(GO:0000245)
mRNA Splice Site Selection
n=5
(GO:0006376)
Spliceosomal snRNP Assembly
n=4
(GO:0000387)
E
Graf et al
(HEK 293)
Åkerstrand et al
(B cell precursors)
Missios et al
(BE(2)-C neuroblastoma)
81
32
1055
58
67
382
1861
F
Åkerstrand
Graf Overlap
Missios Overlap
All studies Overlap
Cytoplasmic Translation
Ribosomal Small Subunit Biogenesis
RNA Export from Nucleus
mRNA Export from Nucleus
Maturation of SSU-rRNA
Maturation of SSU-rRNA
Aerobic Electron Transport Chain
Spliceosomal Complex Assembly
mRNA Splice Site Selection
Spliceosomal snRNP Assembly
FDR
< 0.001
< 0.01
< 0.05
Enrichment
20
30
40
50

Figure 2

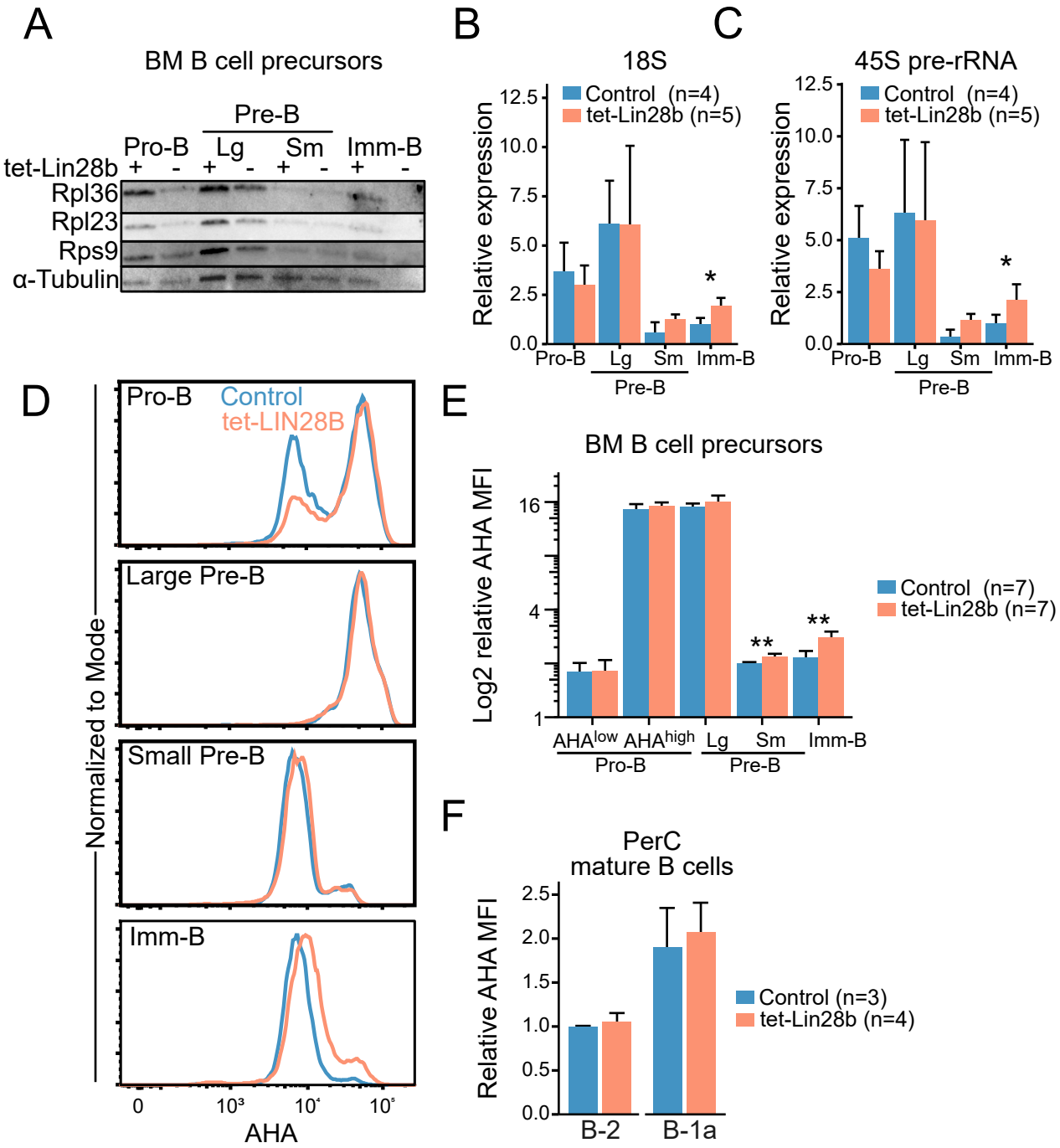
A
BM B cell precursors
Pre-B
Pro-B
Lg
Sm
Imm-B
tet-Lin28b + - + - + - + -
Rpl36
Rpl23
Rps9
α-Tubulin
B
18S
Control (n=4)
tet-Lin28b (n=5)
Relative expression
12.5
10.0
7.5
5.0
2.5
0.0
*
Pro-B
Lg
Sm
Imm-B
Pre-B
C
45S pre-rRNA
Control (n=4)
tet-Lin28b (n=5)
Relative expression
12.5
10.0
7.5
5.0
2.5
0.0
*
Pro-B
Lg
Sm
Imm-B
Pre-B
D
Pro-B
Control
tet-LIN28B
Large Pre-B
Small Pre-B
Imm-B
Normalized to Mode
0
10³
10⁴
10⁵
AHA
E
BM B cell precursors
Log2 relative AHA MFI
16
4
1
**
**
AHAlow
AHAhigh
Lg
Sm
Imm-B
Pro-B
Pre-B
Control (n=7)
tet-Lin28b (n=7)
F
PerC
mature B cells
Relative AHA MFI
2.5
2.0
1.5
1.0
0.5
0.0
B-2
B-1a
Control (n=3)
tet-Lin28b (n=4)

Figure 3

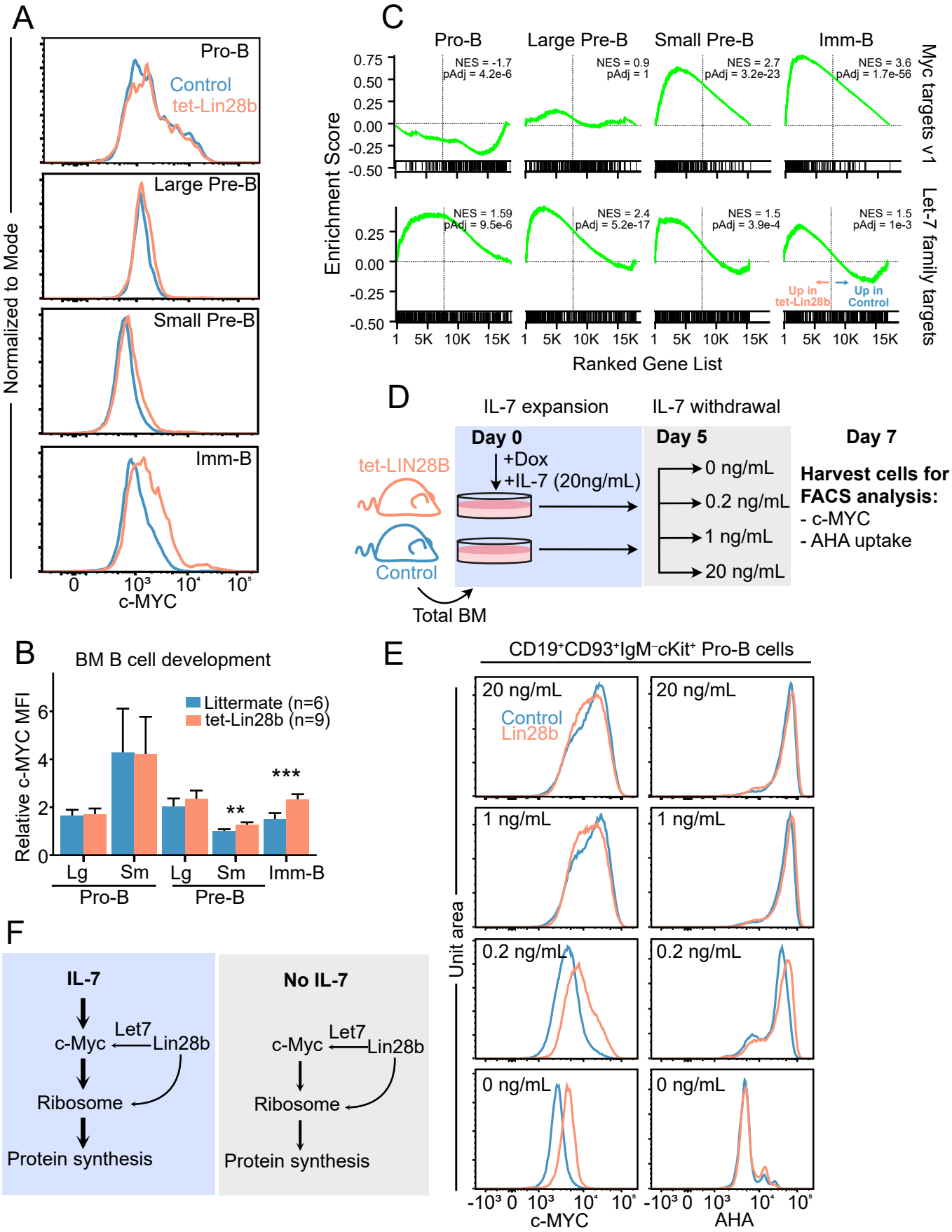
A
Pro-B
Control
tet-Lin28b
Large Pre-B
Small Pre-B
Imm-B
Normalized to Mode
0
10³
10⁴
10⁵
c-MYC
C
Pro-B
Large Pre-B
Small Pre-B
Imm-B
NES = -1.7
pAdj = 4.2e-6
NES = 0.9
pAdj = 1
NES = 2.7
pAdj = 3.2e-23
NES = 3.6
pAdj = 1.7e-56
Myc targets v1
NES = 1.59
pAdj = 9.5e-6
NES = 2.4
pAdj = 5.2e-17
NES = 1.5
pAdj = 3.9e-4
NES = 1.5
pAdj = 1e-3
Up in tet-Lin28b
Up in Control
Let-7 family targets
Enrichment Score
0.75
0.50
0.25
0.00
-0.25
-0.50
1
5K
10K
15K
Ranked Gene List
D
IL-7 expansion
IL-7 withdrawal
Day 0
Day 5
Day 7
tet-LIN28B
+Dox
+IL-7 (20ng/mL)
0 ng/mL
0.2 ng/mL
1 ng/mL
20 ng/mL
Harvest cells for FACS analysis:
- c-MYC
- AHA uptake
Control
Total BM
B
BM B cell development
Littermate (n=6)
tet-Lin28b (n=9)
Relative c-MYC MFI
0
2
4
6
**
***
Lg
Sm
Lg
Sm
Imm-B
Pro-B
Pre-B
E
CD19⁺CD93⁺IgM⁻cKit⁺ Pro-B cells
20 ng/mL
Control
Lin28b
1 ng/mL
0.2 ng/mL
0 ng/mL
Unit area
-10³ 0 10³ 10⁴ 10⁵
c-MYC
AHA
F
IL-7
c-Myc
Let7
Lin28b
Ribosome
Protein synthesis
No IL-7
c-Myc
Let7
Lin28b
Ribosome
Protein synthesis

Figure 4

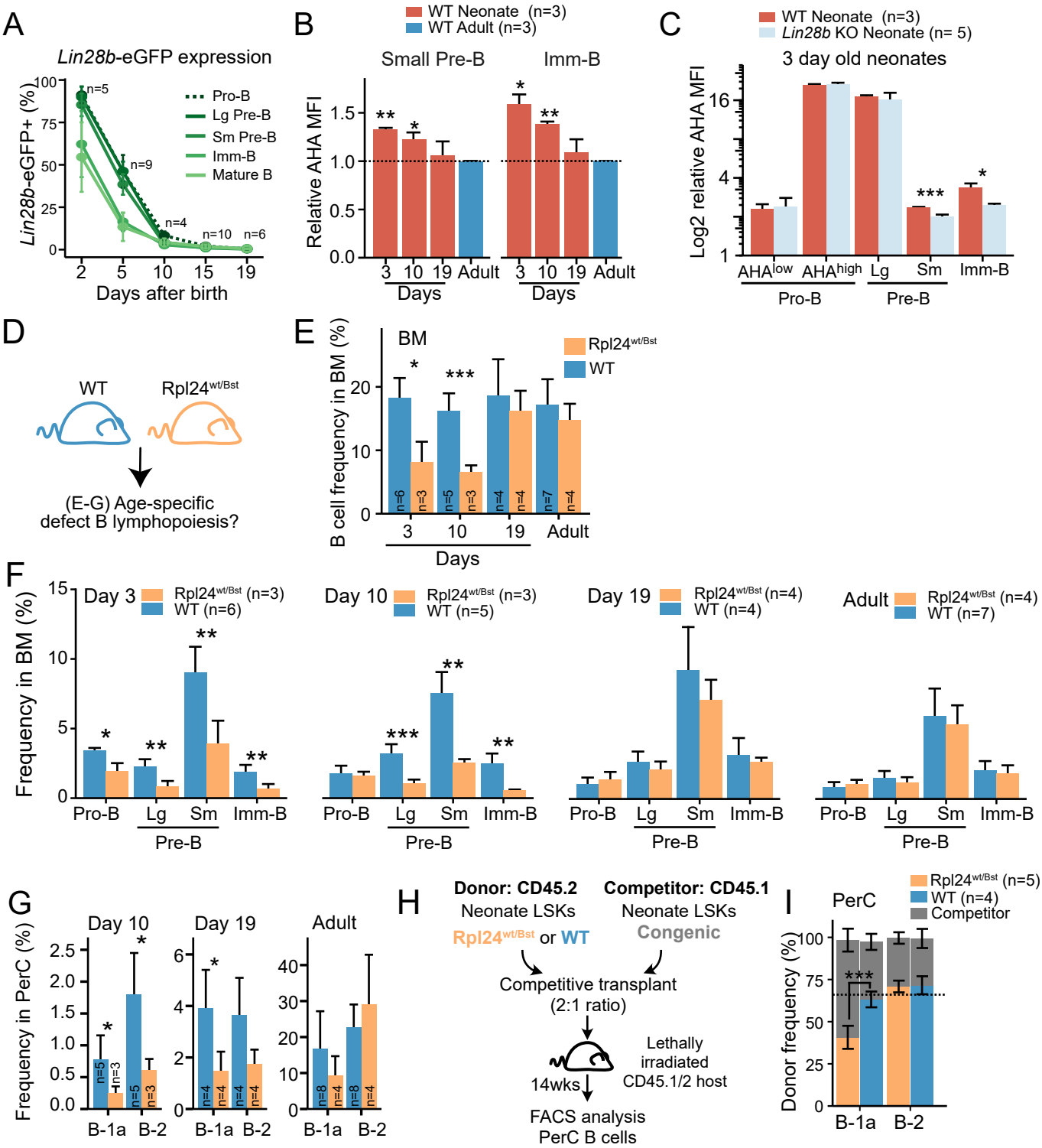
A
Lin28b-eGFP expression
Lin28b-eGFP+ (%)
Pro-B
Lg Pre-B
Sm Pre-B
Imm-B
Mature B
n=5
n=9
n=4
n=10
n=6
Days after birth
B
WT Neonate (n=3)
WT Adult (n=3)
Small Pre-B
Imm-B
Relative AHA MFI
Days
C
WT Neonate (n=3)
Lin28b KO Neonate (n= 5)
3 day old neonates
Log2 relative AHA MFI
AHAlow
AHAhigh
Lg
Sm
Imm-B
Pro-B
Pre-B
D
WT
Rpl24wt/Bst
(E-G) Age-specific defect B lymphopoiesis?
E
BM
Rpl24wt/Bst
WT
B cell frequency in BM (%)
Days
F
Day 3
Rpl24wt/Bst (n=3)
WT (n=6)
Day 10
Rpl24wt/Bst (n=3)
WT (n=5)
Day 19
Rpl24wt/Bst (n=4)
WT (n=4)
Adult
Rpl24wt/Bst (n=4)
WT (n=7)
Frequency in BM (%)
Pro-B
Lg
Sm
Imm-B
Pre-B
G
Day 10
Day 19
Adult
Frequency in PerC (%)
B-1a
B-2
H
Donor: CD45.2
Neonate LSKs
Rpl24wt/Bst or WT
Competitor: CD45.1
Neonate LSKs
Congenic
Competitive transplant
(2:1 ratio)
Lethally irradiated CD45.1/2 host
14wks
FACS analysis
PerC B cells
I
PerC
Rpl24wt/Bst (n=5)
WT (n=4)
Competitor
Donor frequency (%)
B-1a
B-2

Figure 5

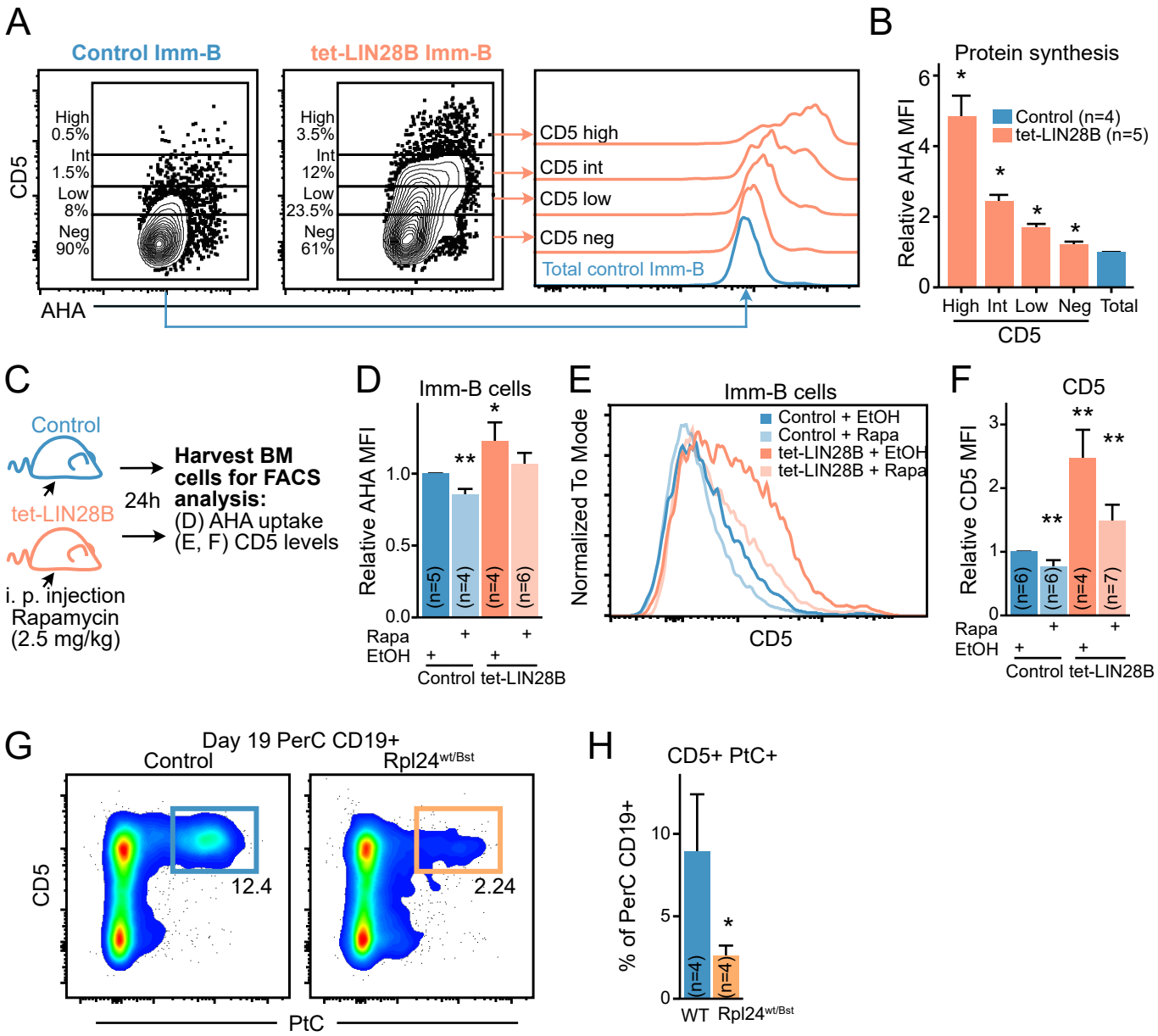
A
Control Imm-B
tet-LIN28B Imm-B
CD5
High 0.5%
Int 1.5%
Low 8%
Neg 90%
High 3.5%
Int 12%
Low 23.5%
Neg 61%
AHA
CD5 high
CD5 int
CD5 low
CD5 neg
Total control Imm-B
B
Protein synthesis
Relative AHA MFI
Control (n=4)
tet-LIN28B (n=5)
High Int Low Neg Total
CD5
C
Control
tet-LIN28B
24h
Harvest BM cells for FACS analysis:
(D) AHA uptake
(E, F) CD5 levels
i. p. injection
Rapamycin
(2.5 mg/kg)
D
Imm-B cells
Relative AHA MFI
(n=5) (n=4) (n=4) (n=6)
Rapa
EtOH
Control tet-LIN28B
E
Imm-B cells
Normalized To Mode
Control + EtOH
Control + Rapa
tet-LIN28B + EtOH
tet-LIN28B + Rapa
CD5
F
CD5
Relative CD5 MFI
(n=6) (n=6) (n=4) (n=7)
Rapa
EtOH
Control tet-LIN28B
G
Day 19 PerC CD19+
Control
Rpl24wt/Bst
CD5
12.4
2.24
PtC
H
CD5+ PtC+
% of PerC CD19+
(n=4) (n=4)
WT Rpl24wt/Bst